MESOSCALE INSTABILITY OF A BAROCLINIC BASIC FLOW —PART II: TRANSVERSAL INSTABILITY

Zhang Kesu (张可苏)

Institute of Atmospheric Physics, Academia Sinica, Beijing

Received August 1, 1987

ABSTRACT

This is the second part of "Mesoscale Instability of a Baroclinic Basic Flow" which discusses the instability of a basic flow against mesoscale perturbations of transversal type.

A bi-mode instability spectrum is obtained by generalizing the Eady model to ageostrophic regime in an f-plane: Eady modes present at the synoptic and subsynoptic scales, while the ageostrophic baroclinic mesoscale modes present at the inertial scales of a few tens to hundreds kilometers. The mesoscale mode is featured by an asymmetric "cat eyes" pattern in the vertical cross section and by an alternative distribution of divergence and vorticity in the horizontal direction. The growth rates of the mesoscale modes are about four times larger than those of Eady modes in magnitudes for the same wind profile. The major energy source for development both Eady mode and mesoscale mode is the baroclinic available energy stored in the rotational basic flow.

I. INTRODUCTION

The previous research on instability of a basic flow against disturbances of the transversal type is mostly concentrated on synoptic and convective scales. Charney (1947) and Eady (1949) first discovered the instability of a baroclinic flow against quasi-geostrophic perturbation of synoptic scales. In the quasi-geostrophic framework a preferred scale about 2000 km may be obtained when extending the spectrum of Eady mode to the shorter wave range by including condensation heating in the model so as to decrease the effective static stability. An Eady mode of shorter wavelength may also be obtained when the wind shear is concentrated within a shallow layer or the basic flow has a significant curvature (Prakki et al., 1982). These "wet" or "shallow" quasi-geostrophic disturbances may be able to interpret the medium-scale waves observed on the "Meiyu" fronts and those short waves around a polar vortex, but the more difficult problem is the dynamics of meso-β systems on the inertial scales (a few tens to hundreds of kilometers). By approximate analyses Stone (1966, 1970) showed that there exist baroclinic instability for Richardson number $R_i>0.95$, symmetric instability for $R_i<0.95$, and Kelvin-Helmholtz instability for $0<R_i<0.25$. Based on the theory of two-dimensional turbulence, Lilly (1983) suggested that the mesoscale motions are supported by small scale motions because the mesoscale motions are located at the inertial regime on the energy spectrum where no energy injection occurs and only energy transfer among different scales are possible. On the other hand, the lack of peak on mesoscales in the statistical power spectrum does not necessarily mean that the atmosphere is absolutely stable against mesoscale perturbations, rather, it may imply that the mesoscale instability requires more rigid criteria and therefore only occurs in the atmosphere with small probability. In order to discover a disturbance on the scales about a hundred kilometers it requires to organize special field experiments with high quality and high temporal and spatial resolutions in observation.

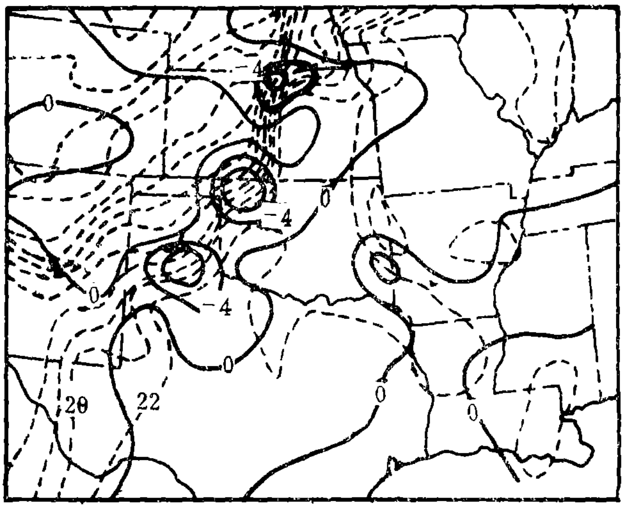

Fig. 1. Distribution of surface mesoscale convergence (solid lines) and temperature waves(dashed lines) along the direction of thermal wind. The contour intervals of the isoplethes are $4\times10^{-5}s^{-1}$ for divergence and 2°C for temperature (1400 GMT 9 May 1979, Texas).

Fig. 1 shows a case of mesoscale analysis based on observations in SESAME 1979 in United States (Ogura et al., 1982). Along the cold front there are temperature waves and divergence disturbances of a wavelength about 400 km. The vorticity also has a corresponding distribution. The wave train aligns along the axis of the south-west jet ahead of a cold vortex on 500 hPa. In the following section the conditions favorable to these kinds of transversal mesoscale disturbances to occur in a baroclinic, continuously stratified atmosphere will be discussed.

II. GOVERNING EQUATIONS AND SIMPLE ANALYTIC SOLUTION

The three-dimensional governing perturbation equations (1) and the set of equations (2) presented in the first part of the present work (Zhang, 1988) are suitable to be solved by matrix method. In order to find the theoretical solution of the problem for a simple wind profile, we first discuss the characteristic equation for transversal disturbances, i. e., Eq. (5) in the first part of the present work:

$$[f^2-k^2(U-c)^2]\frac{d^2W}{dz^2}-\frac{2f^2U_z}{(U-c)}\cdot\frac{dW}{dz}-k^2[N^2-\lambda k^2(U-c)^2 -U_{zz}(U-c)]W=0, \tag{1}$$

where W represents the eigenfunction of the vertical velocity, c the complex characteristic phase speed, U stands for the basic flow, f is the Coriolis parameter, N the buoyancy frequency, k the wavenumber in x-direction, $\lambda=0$ or 1 indicates if the model is hydrostatic or not. Eq. (1) has three singularities on the real axis: $U=c$ and $U=c\pm f/k$, which correspond to three critical levels belonging to Rossby wave and inertial waves, respectively. Eq. (1) becomes quasi-singular when the imaginary part of c is very small which results in difficulties in convergence for computation of c. If $\lambda=0$ and without considering U_{zz}, the problem is relatively easy to handle. Further, for large scale motions k is small, Eq. (1) is reduced to the classical Eady model with only one singularity

$$(U-c)\left[\frac{d^2W}{dz^2}-\frac{k^2N^2}{f^2}W\right]-2U_z\frac{dW}{dz}=0. \tag{2}$$

This model has the theoretical solution and its instability spectrum has a short wave cut-off. Does there exist any mesoscale instability beyond the short wave cut-off? The ageostrophic model (1) may include this possibility. The following analysis will demonstrate the existence of the theoretical solution for the ageostrophic model (1).

By introducing a new variable $R=k(U-c)/f$ and Richardson number $R_i=N^2/U_z^2$ for U_{zz} and $\lambda=0$ Eq. (1) is reduced to the following form

$$R(R^2-1)\frac{d^2W}{dR^2}+2\frac{dW}{dR}+RR_iW=0. \tag{3}$$

It is shown that Eq. (3) is essentially identical with the hypergeometric differential equation. In the canonical form of the hypergeometric differential equation

$$x(x-1)y''+[(\alpha+\beta+1)x-\gamma]y'+\alpha\beta y=0, \tag{4}$$

we introduce variable transformation $x=R^2$, and choose $(\alpha,\beta)=1/2(-1/2\pm\sqrt{1/4-R_i})$, and $\gamma=1/2$, then Eq. (4) is reduced to (3). Therefore Eq. (3) also has a solution in the form of hypergeometric function $F(\alpha, \beta, \gamma, R^2)$. In order to find the specific solution satisfying the upper and lower boundary conditions and to obtain the eigenvalue c, two linearly independent hypergeometric functions F_1 and F_2 are used to construct the general solution

$$W=AF_1+BF_2. \tag{5}$$

The solution W has to satisfy the following relations at the upper and the lower boundaries where $R_T=k(U_T-c)/f$ and $R_B=k(U_B-c)/f$:

$$\left.\begin{aligned}W_T=AF_1(R_T^2)+BF_2(R_T^2)=0\\ W_B=AF_1(R_B^2)+BF_2(R_B^2)=0\end{aligned}\right\}. \tag{6}$$

The eigenvalue c is calculated by the following determinant if the coefficients A and B do not vanish simultaneously:

$$F_1(R_T^2)F_2(R_B^2)-F_2(R_T^2)F_1(R_B^2)=0. \tag{7}$$

This transcendental equation can be solved for eigenvalue c in terms of iterative method.

III. INSTABILITY OF AN IRROTATIONAL STRATIFIED FLOW AND THE "CAT EYES" PATTERN

$f=0$ is one of the special cases of Eq. (1). For the linear wind profile $U=az$ Eq. (1) is reduced to

$$\frac{d^2W}{dz^2}+\left[\frac{R_i}{(z-z_c)^2}-\lambda k^2\right]W=0, \tag{8}$$

where $R_i=N^2/a^2$, $z_c=c/a$. Assuming that $\lambda=0$ and introducing variable transformation $\eta=k(z-z_c)$ we have

$$W=\eta^{1/2}\begin{cases}C_1\cos(b\ln\eta)+C_2\cos(b\ln\eta) \\ C_1\eta^b+C_2\eta^{-b} \\ C_1+C_2\ln\eta\end{cases} \quad \text{when} \quad b^2=\begin{cases}R_i-\dfrac{1}{4} \\ \dfrac{1}{4}-R_i \\ 0\end{cases}$$

where b^2 is defined as an integer. The eigenvalue c is then determined by the upper and lower boundary conditions $W=0$. Assuming that the wind speed at the upper boundary is U_T, for $R_i<1/4$ a complex phase speed $c=U_T/2\ [1+i\,\mathrm{ctg}\,(n\pi/2b)]$ is obtained (n is a positive integer), which causes instability of the basic flow; for $R_i=1/4$ the boundary condition gives $c=U_T/2$; for $R_i>1/4$ we have $c=U_T/(1\text{-}e^{2n\pi/b})$, also representing a neutral wave. Therefore $R_i=1/4$ is a critical value for instability to occur in a hydrostatic basic flow of linear profile.

For nonlinear wind profile Eq. (1) is reduced to Taylor-Goldstein equation:

$$\frac{d^2W}{dz^2}+\left[\frac{N^2}{(U-c)^2}-\frac{U_{zz}}{U-c}-\lambda k^2\right]W=0, \tag{9}$$

which is widely used for discussions of the development and propagation of the gravity

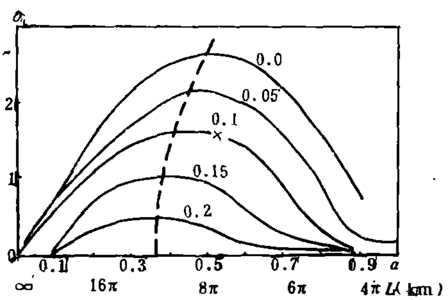

Fig. 2. Instability spectrum in growth rates versus wavelengths and the non-dimensional wavenumber $a=kh$. R_i is labeled near the curves, the bold dashed line indicates the wavelength of the most unstable mode.

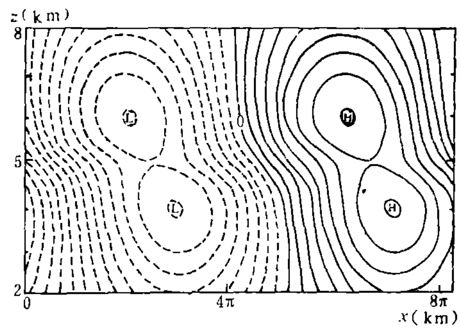

Fig. 3. The eigenfunction corresponding to the point "×" in Fig. 2, is shown in the vertical cross section, height z versus horizontal distance x. $R_i=0.1$, $L=8$ km.

waves. We assume that the basic flow $U=U_0\tanh\ [(z\text{-}z_0)/h]$, and choose the stratification parameter so that the local Richardson number around z_0 is $R_i=0$—0.2 and the vertical resolution $d=20$ m within the integration domain between 0—10 km. In order to obtain a complete picture the center z_0 of the maximum shear is assumed to locate at the center of the integration domain with a characteristic thickness of the shear layer $h=2$ km. The eigenvalue c and the eigenfuntion W satisfying Eq. (9) and the boundary condition $W=0$ are then obtained by "shooting method" (Figs. 2 and 3). Since streamfunction is related to W by $W=\psi_x$, Fig. 3 also represents the picture of the streamfunction satisfying Eq. (9) but with a phase shift of $\pi/2$.

It is realized from the instability spectrum given in Fig. 2 that the whole wavebands of $2\pi h<L<\infty$ are all unstable for a hypertangent basic flow of curvature and with a minimum $R_i=0$—0.1 at $z=z_0$. The maximum growth rate on the instability spectrum locates near the nondimensional wavenumber $kh=0.5$ (wavelength $4\pi h$) with a phase speed $C_r=0$. A "cat eyes" pattern of the streamlines sets up which is centered at the middle level z_0 where the shear reaches its maximum (Fig. 3). As the characteristic thickness of the shear layer h increases, the wavelength of the most unstable mode may increase to a few tens of kilometers which is much larger than the convective scales. For the purpose of comparison, the case for $R_i<0$ is also calculated. The characteristic flow pattern is featured by simple convective cells with a little tilt (figure ommitted) which is more similar to the simple thermal convection rather than the "cat eyes" pattern occurring in a statically stable stratified fluids.

IV. $f\neq 0$ ——EADY MODES AND MESOSCALE MODES

The Coriolis parameter f is usually not negligible for motions on the scale of hundred kilometers. The gradient of temperature supported by rotation of the basic flow may provide available potential energy to the disturbances of certain special structures. The analyses on symmetric instability show that a baroclinic basic flow which is absolutely inertially stable for a pure horizontal disturbance and convectively stable for a vertical perturbation, may be unstable for a slant convective perturbation as long as the disturbance is less tilt than the isentropic surface (Zhang, 1988). For disturbances of transversal type on the synoptic scales the quasi-geostrophic Eady modes and Charney modes are growing with time with their phases tilted westward with height (Charney, 1947; Eady, 1949). The analysis in Section II pointed out that on the wavebands, where ageostrophic wind is important, Eq. (1) has a solution in form of hypergeometric functions. Because solving the transcendental equation (7) by iterative method is time consuming, the following will give the results obtained by two numerical techniques, i. e., the matrix method and shooting method for the phase speeds, growth rates and the characteristic flow patterns.

For a simple transversal perturbation in (x,z)-plane the streamfunction ψ can be introduced to decrease the order of the equation. Let $u=\psi_z$, $w=-\psi_x$, $M^2=-g\partial\ln\bar{\theta}/\partial z$, $N^2=g\partial\ln\bar{\theta}/\partial y$, operater $\nabla^2=\partial^2/\partial x^2+\partial^2/\partial z^2$, and the basic flow be a function of z alone and anelastic assumption is used, the perturbation equations are then written as

$$\left.\begin{aligned}&\left(\frac{\partial}{\partial t}+U\frac{\partial}{\partial x}\right)\nabla^2\psi-U_{zz}\psi_x-fv_z+\theta_x=0,\\&\left(\frac{\partial}{\partial t}+U\frac{\partial}{\partial x}\right)v+f\psi_z=0,\\&\left(\frac{\partial}{\partial t}+U\frac{\partial}{\partial x}\right)\theta-M^2v+N^2\psi_x=0.\end{aligned}\right\}\tag{10}$$

Assuming the following characteristic wave solution

$$(\psi,v,\theta)=Re[(\Psi,V,T)e^{ik(x-ct)}]\tag{11}$$

and substituting (11) for (10), a set of ordinary differential equations in z are then obtained for eigenfunctions (Ψ,V,T), which are further discretized in z to produce a matrix equation

$$c\mathscr{P}\xi=\mathscr{Q}\xi\tag{12}$$

where c is the eigenvalue, ξ the eigenvector defined by discrete point sets on z coordinate,

$\mathscr{P}$ and $\mathscr{Q}$ the complex matrices consisting of the parameters of the basic flow M^2, N^2, f, the wavenumber k and the vertical resolution d. Under the constraints of the upper and lower boundary condition $W=0$, Eq. (12) can be directly solved by use of the standard computer software.

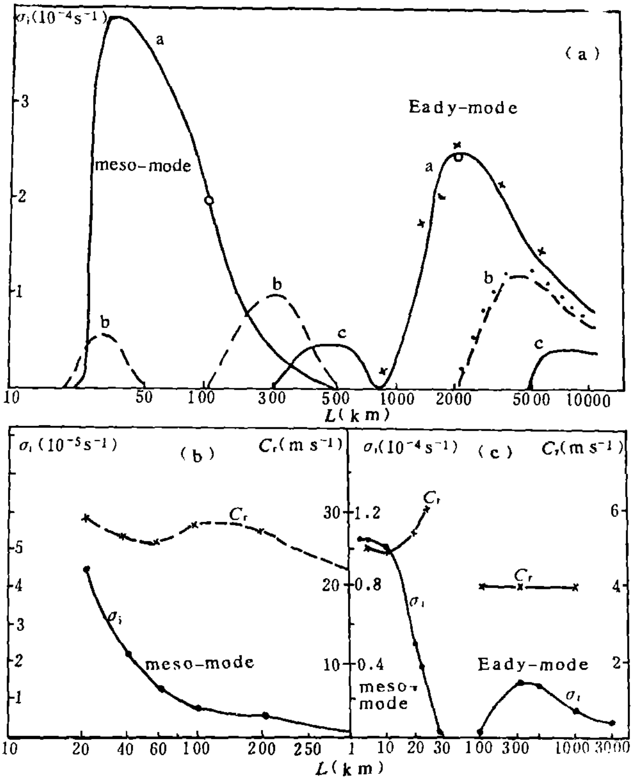

Fig. 4. (a) The instability spectral curves a, b, c are for the baroclinic flow with $R_i=0.625$, 6.25 and 25, respectively. The set of curves on the right hand side represents Eady modes, while that on the left side represents mesoscale modes, $d=0.5$ km, the extent of the basic flow and the integration domain $H=10$ km, $U=0$—40 m/s.

(b) The growth rates and phase speeds of mesoscale modes (notice that the units of the coordinate are 10 times larger than that used in Fig. 4a) $R_i=0.625$, $H=10$ km, $d=0.25$ km, $U=0$—40 m/s.

(c) The growth retes and phase speeds for mesoscale modes and Eady modes. $R_i=0.625$, $H=2$ km,. $d=0.05$ km, $U=0$—8 m/s. The abscissa indicates wavelength, units in km.

Fig. 4 shows the instability spectra obtained by matrix method for $R_i=0.625$, 6.25 and 25 ($U_{zz}=0$). The speed of the basic flow linearly increases from 0 to 40 m/s within the integration domain $z=0$—10 km. A staggering scheme is used for arrangement of v, θ and ψ with $d=0.5$ km and 0.25 km for 20 and 40-level model, respectively. The sets of modes are obtained from the calculations: Eady modes and mesoscale inertial gravity modes. The group of curves on the right hand side in Fig. 4a indicates the growth rates of Eady modes. As R_i decreases the instability spectra shift to the left ("violet shift") with a shortened wavelength and an enhanced growth rates $\sigma_i=kc_i$. In order to verify the accuracy of the matrix method the theoretical solution of Eady model is also computed for the same parameters (Eady, 1949). The growth rates are shown in Fig. 4a by those points which are close to the curve b. This implies a sufficient accuracy of the matrix method for calculation of Eady mode in a 20-level model. The truncation wavelength of curve a is about 1000 km for $R_i=0.625$ and the maximum growth rate, which corresponds to an e-folding time around 12 hours, appears at the wavelength about 1880 km. According to Tokioka's estimate (1971), the magnitude of R_i on the Meiyu front is about 0.4. He obtained a wavelength of maximum growth rate about 1256 km in a 30-level model for a basic flow of $R_i=0.4$ and a shear layer of 4 km in its vertical extent. The results of the computation obviouly depend upon R_i and the thickness H of the shear layer. In order to check the accuracy of computation for curve a, the shooting method of high resolution ($d=10$ m) is also used to solve the two-point boundary value problem of Eq. (1) by use of curve a as the initial guess. The calculated growth rates for the same parameters are marked in Fig. 4a by "×", which are very close to the results of 20-level model solved by matrix method. This indicates that the vertical resolution for calculations of Eady-mode is sufficient within the range of meso-α scales.

It is interesting to notice some similarities of the above results to those in computation of geostrophic modes. Kuo (1979) has obtained more than one set of instability spectra for the growing ultra-long waves beyond the longwave cut-off of Charney modes. In the above calculations more than one set of mesoscale ageostrophic instability spectra beyond the short wave cut-off of Eady-modes is also obtained as shown in Fig. 4a. Especially, when R_i is smaller than one, the whole meso-β scales ranging from 20—500 km are all unstable. Unlike Eady-modes, the computation on mesoscale bands is extremely sensitive to the vertical resolution. The integration domain of Eq. (1) contains only one singularity at synoptic scales but includes three singularities at mesoscales, which correspondingly requires high resolution in the vertical. A series of numerical experiments of different resolutions for $R_i=0.625$ show that the simplest two-level model is able to produce Eady-modes, but it loses mesoscale instability at all. The five-level model can produce weak instability on mesoscales. The 20-level model further results in a significant instability spectrum at mesoscales as shown in Fig. 4a. In a 40-level model the computed σ_i is greatly increased with a maximum value shifted towards the shorter waves. There is no short wave cut-off at the wavelength about 20 km, which occurred in the 20-level model as a computational cut-off. The e-folding time given by the 40-level model is about 3—4 hours, corresponding to a σ_i much larger than that of Eady-mode. The phase speeds are between 20—30 m/s, higher than the vertically averaged wind speed. According to Kuo's experience (1985), the solution has little changes when the number of levels changes between 50—100, implying that the solution is approaching convergence. In order to further clarify the impact of the vertical resolution on computations at mesoscales without increasing the requirement for core storage of computers, the 40-level model is still used but with a smaller vertical domain of 2 km and a resolution $d=0.05$ km which is 10 times higher than that used in Fig. 4a. The results are shown in Fig. 4c. The bi-mode instability spectrum is again obtained with its left hand side representing the mesoscale modes and the right hand side the ageostrophic Eady modes occurring on the mesoscales. The computational short wave cut-off no longer appears because of the increased resolution. The behavior of σ_i approaching to saturation bears a similarity to the spectral behavior of the symmetric instability. Moreover, the spectra of Eady-modes and the mesoscale modes all shift to the short wave side since the vertical extent of the shear layer has been significantly reduced. In case of low resolution ($d=0.5$ km) the growth rate on mesoscales is about 1.5 times larger than that of the Eady modes in their maximum values (Fig. 4a). In case of high resolution ($d=0.05$ km) the maximum growth rate of the ageostrophic mesoscale modes is about 3.6 times larger than that of Eady modes at synoptic scales. Such a large growth rate is necessary for the development of mesoscale disturbances.

It is at least of some confidence from the above calculations at different resolutions that there exist "shallow" or "moist" Eady modes at the meso-α scales (for small H and R_i), and the ageostrophic inertial gravity modes at the inertial scales from tens to hundreds of kilometers.Their growth rates are smaller than those of convections in a static unstable atmosphere but are larger than those of the quasi-geostrophic Eady-modes.

V. STRUCTURE OF THE CHARACTERISTIC WAVE AND ENERGY CONVERSION

The property of energy conversions can be determined from the structures of the characteristic waves and of the baroclinic basic flow. In a shear flow without rotation the kinetic energy of the basic flow is the unique source of energy for the development of the disturbances; while in a shear flow with rotation the available potential energy supported by the rotation of the system can be another major source of energy for the growth of the disturbances. The previous investigations show that Eady-modes on synoptic scales are supported by the latter source, whereas the small scale instability of a shear flow is supported by the former source. This section will analyze the structure of the characteristic waves and the energy sources for the growing disturbances on mesoscales. The formulas for energy calculation have been given in the first part of the present paper (Zhang, 1988).

The structure of Eady mode of wavelength 2000 km is shown in Fig. 5 for $R_i=0.625$ (corresponding to the point o in Fig. 4a). The eigenfunction and eigenvalue are simultaneously obtained by solving Eq. (12). Fig. 5 delineates the major feature of Eady mode: the vertical velocity reaches its maximum in the middle level, the trough line and the ridge line (the lines which separate the southerly and northerly) slant westward with increasing height. The temperature disturbance has a phase lag in respect to the wind perturbation, v and w are positively correlated while u and w have a negative correlation. Substituting the solution of the characteristic wave into the energy equations, we obtain the ratio $r=\langle\bar{P},P'\rangle/\langle\bar{K},K'\rangle$ which is about 100, implying that the Eady-modes are baroclinically dominated in nature.

Fig. 6 shows the structure of the ageostrophic mesoscale mode with wavelength 100 km (the point o in Fig. 4a), the bold solid and dashed lines represent streamfunction in the (x,z)-plane, as a whole which is similar to the "cat eyes" flow pattern obtained in an irrotational shear flow with $f=0$ (Fig. 3), except that the disturbances are more concentrated in the lower layer, especially with a rapid decreasing of v and θ' with height. Recently,

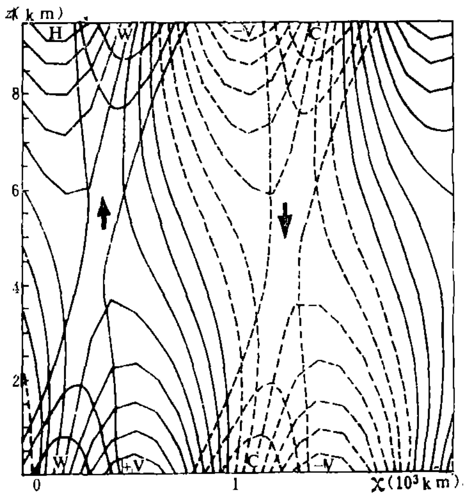

Fig. 5. The structure of the Eady-mode in (x, z)-plane. The bold solid and dashed lines are isopleths of souther and norther wind speeds, the thin lines are for the positive and negative temperature perturbations, respectively (units are arbitrary). The maximum ascending and descending motions are marked by the bold arrow. $H=10$ km, $R_i=0.625$, $L=2000$ km (points × in Fig. 4a).

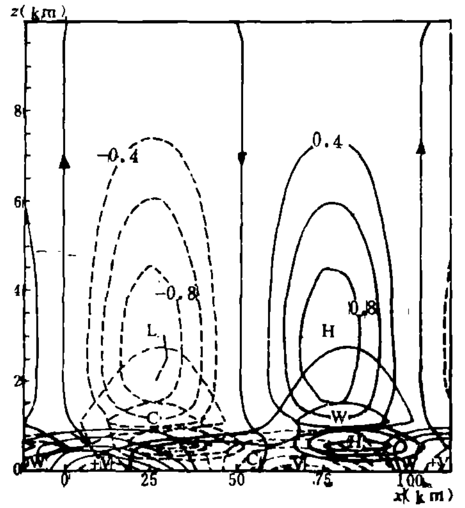

Fig. 6. The structure of the ageostrophic mesoscale eigenmode. The bold, mean and thin lines are the isotaches for streamline, temperature and meridional wind speed, respectively. The solid lines are positive, and the dashed one negative. The positive and negative temperature centers are marked by W,C. $R_i=0.625$, $L=100$ Km (point o in Fig. 4a).

Kuo and Seitter (1985) have also calculated the structures of the disturbances for an atmosphere of partly unstable stratification, which are also featured by a rapid damping of χ and θ with height. The distributions of divergence and convergence can be deduced from streamfunction in Fig. 6 based on $u=\psi_z$ and $w=-\psi_x$, and the vorticity $\zeta=\partial v/\partial x$ may be derived from v. Therefore the following structure sequence in the x-direction is obtained: convergence⟶anticyclone⟶divergence⟶cyclone.

Above the center of the lower "cat eye", convergence changes sign while v keeps its sign to be unchanged, which forms an inversed structure sequence. On the scale of hundreds of kilometers the inertial gravity waves form an alternative distribution of the mesoscale centers of divergence and vorticity because of the effect of f, which may generate mesoscale disturbances of transversal type in the lower troposphere as shown in Fig. 1. A better picture may be obtained when the same calculation is applied to the realistic wind profiles instead of the ideal linear profile.

The energy properties of the ageostrophic mesoscale modes are different from those of Eady-modes. By substituting the eigen solution of Eq. (12) into the energy equations for a wavelength of 100 km, the calculated ratio $r=\langle\bar{P},P'\rangle/\langle\bar{K},K'\rangle$ is about 5, i. e. both terms of energy conversions are of the same order of magnitudes. However, the energy properties are quite different when compared with an irrotational system. In a system without rotation, the conversion term $\langle \bar{P}, P' \rangle = 0$, and hence $r = 0$. This indicates that the mesoscale perturbation is more likely to develop in a baroclinic basic flow than in a fluid system without rotation. The significant positive correlation in (v, θ) and the negative correlation in (u, w) are both favorable to the energy conversions from the basic flow toward the disturbances.

VI. CONCLUDING REMARKS

In order to interpret disturbances propagating along the basic flow on the meso-to-medium scales, Eady model is generalized to ageostrophic regime. The mesoscale instability spectra are found beyond the short wave cut-off of Eady model. Eady-modes may extend to the meso-α wave band, keeping a quasi-geostrophic feature, as long as the vertical extent of the shear layer is small or Richardson number is small. While on the inertial scales of a few tens to hundreds of kilometers, the fastest growing mode possesses the property of the inertial gravity waves with a growth rate about 4 times larger than that of Eady-mode. Such a large growth rate may be able to generate vertical velocity and low level convergence of sufficient intensity, and hence to serve as a dynamic mechanism for triggering and organizing the deep convective clouds.

The present paper is limited to discussing the transversal disturbances of the mesoscales with the simplest model of prototype. In order to interpret the propagating mesoscale disturbances along the "Meiyu" front and along the low level jets as well as the mesoscale gravity waves propagating into the stratosphere and mesosphere from the tropopause jet stream, more calculations on a variety of realistic situations are expected.

REFERENCES

Charney, J.G. (1947), The dynamics of long waves in a baroclinic, westerly currert, *J. Meteor.*, **4**: 35—162.

Eady, E. T. (1949), Long waves and cyclone waves, *Tellus*, **1**: 33—52.

Kuo, H. L. (1979), Baroclinic instabilities of linear and jet profiles in the atmosphere, *J. Atmos. Sci.*, **36**: 2360—2378.

Kuo, H. L. and Seitter, K. L. (1985), Instability of sheering geostrophic currents in neutral and partly unstable atmospheres, *J. Atmos. Sci.*, **42**: 331—345.

Lilly, D. K. (1983), Stratified turbulence and the mesoscale variabiliy of the atmosphere, *J. Atmos. Sci.*, **40**: 749—761.

Ogura, Y. et al. (1982), Possible Triggering mechanisms for severe storms in SESAME-AVE IV (9—10 May 1979), *Bull. Amer. Meteor. Soc.*, **63**: 503—515.

Prakki, S. et al. (1982), Sub-synoptic scale baroclinic instability, *J. Atmos. Sci.*, **39**: 1052—1061.

Stone, P. H. (1966), On Non-geostrophic baroclinic stability, *J. Atmos. Sci*, **23**: 390—400.

Stone, P. H. (1970), On Non-geostrophic baroclinic stability, part II, *J. Atmos. Sci.*, **27**: 721—726.

Tokioka, T. (1971), Supplement to non-geostrophic and non-hydrostatic stability of a baroclinic fluid and medium-scale disturbances on the fronts, *J. Meteor Soc. Japan*, **49**: 129—132.

Zhang Kesu (1988), Mesoscale instability of a basic baroclinic flow——part I: symmetric instability, *Acta Met. S'n.*, **2**: 135—145.